

# Dynamic Hydrogels for Prevention of Post-Operative Peritoneal Adhesions

Lyndsay M. Stapleton, Haley J. Lucian, Abigail K. Grosskopf, Anton A. A. Smith, Kailey P. Totherow, Y. Joseph Woo,\* and Eric A. Appel\*

Post-operative adhesions are fibrous bands of scar tissue formed between internal tissues and organs causing clinical morbidity and their prevention represents a critical unmet need. Over 20 million Americans undergo invasive surgery each year and 95% of those patients develop post-operative adhesions. More specifically, peritoneal adhesions forming as a result of abdominal surgery can result in severe complications such as chronic pain or adhesive small bowel obstruction requiring secondary adhesiolysis surgery. Additionally, adhesiolysis increases operation times during reoperative procedures and increases the risk of hemorrhage and organ injury upon reentry. This work reports the use of a dynamically crosslinked polymer-nanoparticle (PNP) hydrogel adhesion barrier comprised of hydrophobically modified hydroxypropylmethylcellulose and biodegradable PEG-PLA nanoparticles. These materials have desirable viscoelastic and flow properties, long-term physical stability during storage, permit administration via spraying, enable local retention in the abdominal cavity for 2 weeks, and definitively reduce peritoneal adhesion formation. Using a rodent ischemic button model to generate peritoneal adhesions ( $n \geq 4$ ), the PNP hydrogel significantly reduced peritoneal adhesion severity compared to commercial control products when assessed by a standardized 5-point scale ( $3.18 \pm 1.07$  versus  $1.35 \pm 0.63$ ;  $p = 0.0014$ ). These results suggest that the PNP hydrogel adhesion barrier is a simple and effective solution for the prevention of peritoneal adhesions.

form between internal tissues and organs, specifically, the omentum, loops of bowel and the abdominal wall (Figure 1a).<sup>[1]</sup> These adhesions can range in severity, consisting of a thin film of connective tissue, a thick, fibrous bridge with blood vessels and nerve tissue, or direct solid adherence between two internal tissue surfaces.<sup>[2]</sup> Over 20 million Americans undergo invasive surgery each year and adhesions develop after 95% of all operations, regardless of the procedure or location in the body.<sup>[3]</sup> Following abdominal or general surgery, many patients experience significant post-operative adhesion-related complications, such as severe pain and/or organ dysfunction, with 15–30% of patients requiring a second operation to release the adhesions (i.e., adhesiolysis).<sup>[4–8]</sup> Other studies have similarly reported that approximately one-third of abdominal or pelvic surgery patients were readmitted an average of two times over the course of a ten-year study for either symptoms related to adhesions or for a secondary operation that could be complicated by the presence adhesions.<sup>[1]</sup> Additionally, greater than 20% of all readmissions occurred during the first year after initial surgery and 4.5% of these readmissions were for adhesive small bowel


obstruction, a severe complication to post-operative adhesions.<sup>[1]</sup> Furthermore, during reoperations for other indications, requisite adhesiolysis for exposure imparts additional risks upon the patient, including extended operation times, anesthesia, and

## 1. Introduction

Peritoneal adhesions are fibrous bands of scar tissue that arise from normal wound-healing processes following surgery and

L. M. Stapleton, K. P. Totherow, Y. J. Woo, E. A. Appel  
Department of Bioengineering  
Stanford University  
Stanford, CA 94305, USA  
E-mail: joswoo@stanford.edu; eappel@stanford.edu  
H. J. Lucian, Y. J. Woo  
Department of Cardiothoracic Surgery  
Stanford University School of Medicine  
Stanford, CA 94305, USA

A. K. Grosskopf, A. A. A. Smith, E. A. Appel  
Department of Materials Science and Engineering  
Stanford University  
Stanford, CA 94305, USA  
E. A. Appel  
ChEM-H Institute  
Stanford University  
Stanford, CA 94305, USA  
E. A. Appel  
Department of Pediatrics (Endocrinology)  
Stanford University School of Medicine  
Stanford, CA 94305, USA

 The ORCID identification number(s) for the author(s) of this article can be found under <https://doi.org/10.1002/adtp.202000242>

DOI: 10.1002/adtp.202000242

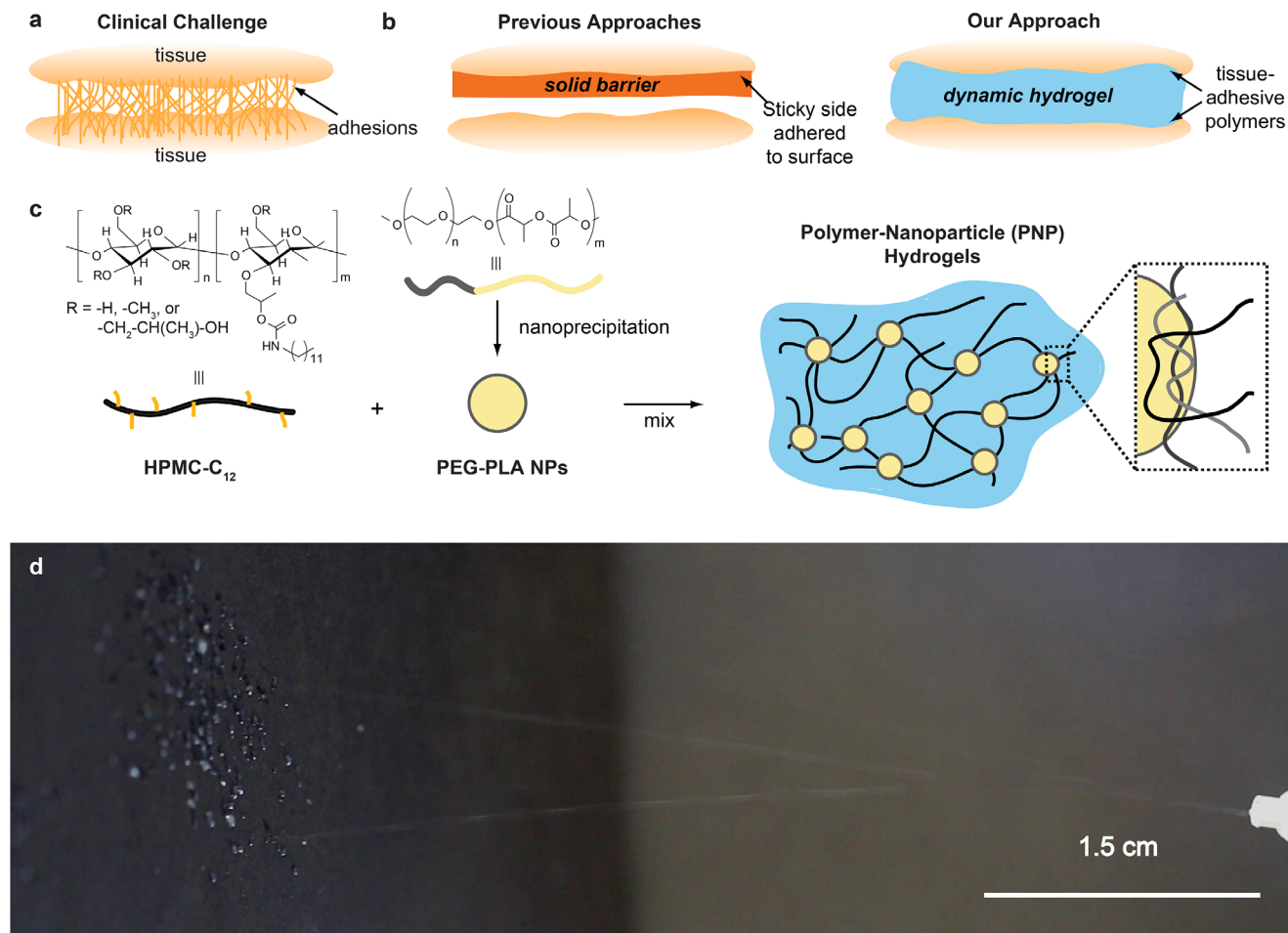


**Figure 1.** a) Schematic representation of adhesion formation between two tissues. b) Schematic representation of previous approaches to prevent adhesions utilizing solid adhesion barriers to physically separate organs and tissues including covalently cross-linked hydrogels formed through in situ polymerization of precursor macromers or the commercially available film, Sefrafilm. Our approach utilizes dynamically crosslinked, shear-thinning, self-healing, and viscoelastic polymer hydrogels that are placed between organs and tissues, allowing these structures to move naturally. c) Our materials exploit multivalent and dynamic non-covalent interactions between hydrophobically modified hydropropylmethylcellulose (HPMC-C<sub>12</sub>) and poly(ethylene glycol)-*block*-poly(lactic acid) (PEG-PLA) to form hydrogels that can be sprayed through standard equipment, adhere to tissue (HPMC-C<sub>12</sub> is tissue adhesive), and provide a viscoelastic barrier between organs and tissues to inhibit adhesion formation. d) Representative snapshot from a video of PNP hydrogel sprayed from standard equipment.

recovery times.<sup>[9]</sup> Patients also have an increased risk of hemorrhage and/or tissue damage including injury to the bladder, enterocutaneous fistulas, and resection of damaged bowel.<sup>[9]</sup> Overall, post-operative adhesions have a substantial impact on the U.S. healthcare system with adhesion treatment costs exceeding 2.5 billion and adhesion related complications resulting in nearly 1 million days of inpatient care (e.g., lost patient wages) each year, representing a significant clinical challenge.<sup>[10]</sup>

Current clinical options for adhesion prevention consist of solid barriers comprised of polymer or hydrogel films made from polysaccharides and/or synthetic polymers (resorbable and non-resorbable varieties) that are designed to physically separate scarring tissue and surrounding organs (Figure 1b). The current standard of care for abdominal surgeries in clinical practice is to i) not utilize an adhesion barrier of any sort, ii) make smaller incisions to try to localize adhesions, albeit often unsuccessfully, and/or iii) utilize a commercially available film (Sefrafilm,

Sanofi/Genzyme) or a woven fabric (Interceed, Ethicon).<sup>[11]</sup> These commercially available treatment options are composed of hyaluronic acid (HA) and carboxymethylcellulose (CMC). In clinical practice, these barriers are often difficult to administer over the target tissues to adequately maintain surface coverage and form an effective physical barrier separating the tissues and organs of interest. Furthermore, these sheet-like barriers have been reported to become easily dislodged on account of natural tissue movement and cannot be made to cover the entire surface of target tissues with irregular surfaces or those that are heavily folded, such as the small intestine, leaving these surfaces vulnerable to potential adhesion formation.<sup>[12]</sup> Research groups have addressed the difficulties associated with the administration of solid barriers through development of sprayable polymer solutions that undergo in situ polymerization via thiol-maleimide or thiol-acrylate Michael addition reactions, amine-aldehyde or oxide-aldehyde imine-forming reactions, or photo-initiated

radical polymerization to form covalent hydrogels with tunable mechanical properties similar to soft biological tissues.<sup>[7,13–20]</sup> However, the irreversibility of the crosslinks in these systems generally makes them brittle and/or unable to accommodate the dynamic movement of tissues inside the body, leaving them susceptible to becoming dislodged and resulting in failure of adhesion prevention.<sup>[21]</sup>

Recently, our team published an innovative approach to the prevention of post-operative adhesions using a supramolecular polymer-nanoparticle (PNP) hydrogel platform that exploits multivalent, non-covalent interactions between hydrophobically modified cellulose derivatives and nanoparticles (NPs) to form robust yet dynamic hydrogels.<sup>[22–24]</sup> These PNP hydrogels are formed by simple mixing of aqueous solutions of dodecyl-modified hydroxypropyl-methylcellulose (HPMC-C<sub>12</sub>) with biodegradable polymeric NPs composed of poly(ethylene glycol)-*b*-poly(lactic acid) (PEG-PLA) (Figure 1c).<sup>[25–28]</sup> Our study demonstrated a significant reduction in post-operative adhesions in small and large animal models of cardiac adhesions establishing a proof-of-concept platform for an effective adhesion barrier technology.<sup>[22]</sup> These materials were also shown to have robust tissue adherence properties enabling sustained local retention relevant to published adhesion formation timeframes and the inability to swell due to the dynamic crosslinks dissipating the stresses that drives swelling typically observed in covalent hydrogel systems.<sup>[22,23,29–31]</sup> Here, we sought to broaden the clinical translatability of these PNP hydrogels, expanding upon the surgical indications that these PNP hydrogels could be used, by exploring the therapeutic benefit of our two top-performing PNP hydrogel formulations in a small animal model of peritoneal adhesions. We hypothesized that our PNP hydrogel platform would demonstrate long-term local retention and a high degree of biocompatibility, while continuing to constitute a distinct alternative approach to address the critical unmet need for a functional adhesion barrier for peritoneal surgery.

## 2. Results

### 2.1. Viscoelastic and Flow Properties of PNP Hydrogel

In our previous study, we investigated a range of physical and mechanical parameters to determine the optimal tissue adhesive PNP hydrogel formulation necessary for robust adhesion prevention following cardiothoracic surgery.<sup>[22]</sup> In the present work, we sought to investigate the mechanical properties of our two top-performing PNP hydrogel formulations, denoted polymer: NP (wt%:wt%, **Figure 2a–g**), for prevention of peritoneal adhesions. Additionally, we investigate the storage stability of the top PNP hydrogel formulation, comprising 1 wt% HPMC-C<sub>12</sub> and 10 wt% PEG-PLA NPs (2:10), over a six-month period under refrigerated conditions (4 °C, **Figure 2h–k**) to further assess potential clinical utility.

The PNP 1:10 and PNP 2:10 hydrogels used in this study maintained solid-like behavior ( $G'$  (storage modulus) >  $G''$  (loss modulus)) and linear viscoelastic responses up to strains exceeding 100% in strain-dependent oscillatory rheological measurements (**Figure 2a**). These results indicate that the solid-like properties of these hydrogels are preserved over a broad range of strains. Fur-

thermore, the PNP 1:10 hydrogel formulation maintained this broad linear viscoelastic regime throughout the 6 months of storage (**Figure 2h**), suggesting a high degree of stability of these PNP hydrogels. We have previously found that PEG-PLA NPs, which are the primary hydrogel component subject to hydrolytic degradation during storage, are stable for months even under stressed aging conditions.<sup>[32]</sup> Moreover, the PNP hydrogel formulations exhibited viscoelastic responses that were highly dependent on formulation, but where both 1:10 and 2:10 formulations nevertheless maintained solid-like behavior over the entire range of observed frequencies ( $\omega = 0.1–100 \text{ rad s}^{-1}$ ). The PNP 1:10 hydrogel retained this frequency response throughout the 6 months of storage (**Figure 2i**), corroborating the observations made above.

Step-strain measurements were performed to demonstrate recovery of the PNP hydrogel dynamic material response following network rupture at high strains. High magnitude strains were applied to break the hydrogel structure ( $\epsilon = 750\%$ ), which was followed by low magnitude strains ( $\epsilon = 0.5\%$ ) to investigate the rate and extent of hydrogel recovery to initial mechanical properties (**Figure 2c**). PNP hydrogels undergo a dramatic change to fluid-like behavior at high strains, indicated by an inversion of  $G'$  and  $G''$ , but rapidly recover (<5 s) their initial solid-like dynamic response when the strain is decreased. Again, this behavior was repeatable over several cycles during each monthly timepoint under 4 °C storage conditions, indicating that the shear-thinning and self-healing nature of these materials is stable for 6 months and is driven by the rupture and recovery of the non-covalent crosslinks (**Figure 2j**).

Steady-shear measurements were performed to investigate the stability of the flow properties associated with the 1:10 and 2:10 PNP hydrogel formulations, which are highly relevant to flow-based processes such as spraying, spreading, or injection (**Figure 2d**). PNP hydrogels also demonstrated retention of their highly shear-thinning nature, reducing their viscosity upwards of three orders of magnitude over shear rates extending from 0.1–100  $\text{s}^{-1}$  over a 6-month period (**Figure 2k**). These results indicate the beneficial mechanical properties of our previously determined top-two PNP hydrogel formulations (1:10 and 2:10) and demonstrate the stability of our previously determined top-performing PNP hydrogel formulation (1:10) which is exceedingly important for the potential translation of this material into a commercially available, anti-adhesion system.<sup>[22]</sup> Finally, we assessed the adhesion of PNP hydrogel formulations to tissue by characterizing the yield stress behavior of the PNP hydrogel on and off tissue (**Figure 2e**). The hydrogel demonstrated similar yield stress whether it was loaded onto the rheometer or onto the tissue, indicative of cohesive yielding behavior (failure of the gel itself) and not adhesive failure between the hypodermis and the hydrogel (**Figure 2f–g**). We hypothesize that the tissue adhesive nature of the PNP hydrogel formulations stems from the known mucous adhesive properties of HPMC, a commonly used excipient in pharmaceutical formulations. These mucous adhesive properties are non-covalent and allow the PNP hydrogel adhesion barrier to adhere in situ without permanently bonding to the tissue of interest. The observed results from yield stress rheology indicated beneficial tissue adherence properties that potentially aid in the local retention of the PNP hydrogel adhesion barrier in the abdomen.

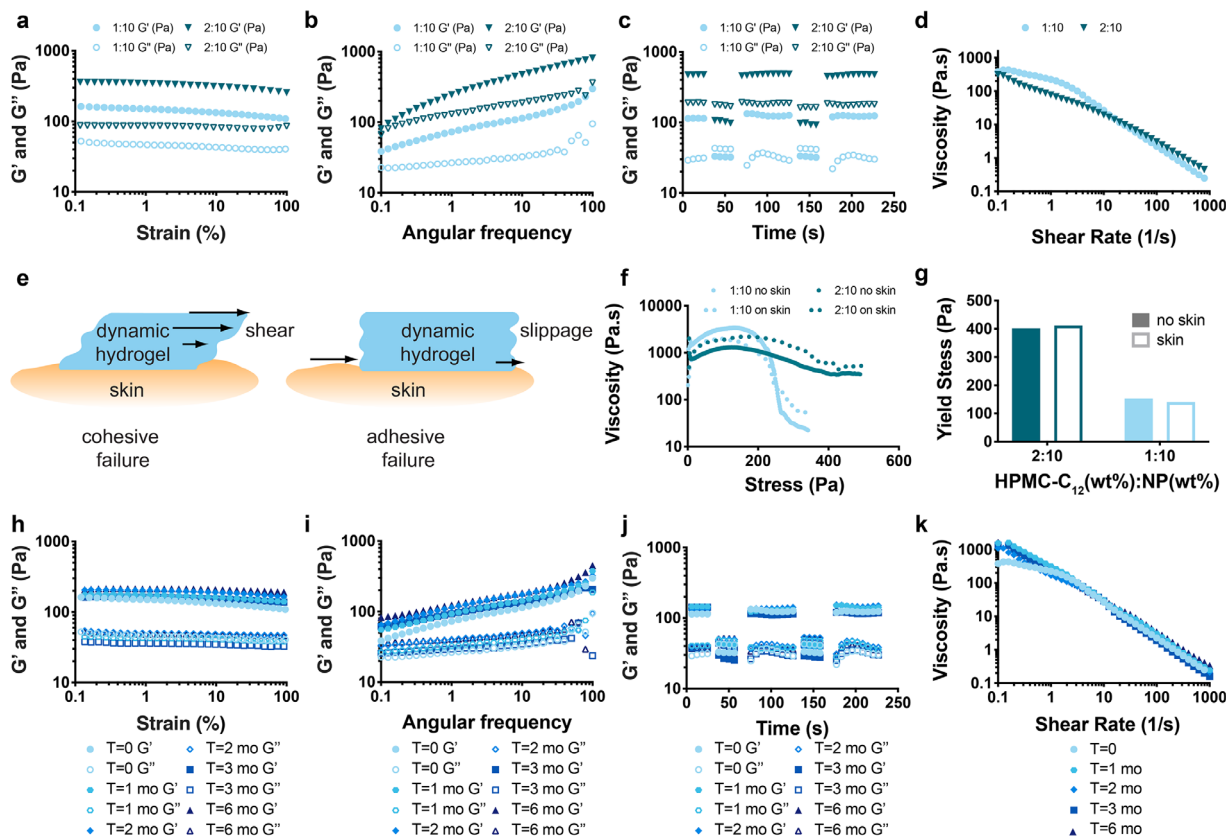


**Figure 2.** a) Strain-dependent ( $\omega = 10 \text{ rad s}^{-1}$ ,  $25 \text{ }^\circ\text{C}$ ) and b) frequency-dependent ( $\epsilon = 2\%$ ,  $25 \text{ }^\circ\text{C}$ ) oscillatory shear rheology of 1:10 and 2:10 PNP hydrogel formulations comprising HPMC- $\text{C}_{12}$  and PEGPLA nanoparticles. c) Step-strain measurements of PNP 1:10 and 2:10 hydrogel formulations with high strains (destructive; 750%) and low strains (restorative; 0.5%) to characterize extent and rate of stationary self-healing. d) Steady-shear rheology of PNP 1:10 and 2:10 hydrogel formulations demonstrating highly shear-thinning behavior. e) Schematic demonstrating adhesive vs. cohesive failure of PNP hydrogel. f) Yield stress behavior of PNP hydrogel in a standard parallel plate geometry and on rat hypodermis in a stress ramp experiment performed at a rate of approximately  $1.5 \text{ Pa s}^{-1}$ . g) Yield stress values of PNP hydrogel obtained from the peak viscosity observed in the stress ramp. h) Strain-dependent ( $\omega = 10 \text{ rad s}^{-1}$ ,  $25 \text{ }^\circ\text{C}$ ) and i) frequency-dependent ( $\epsilon = 2\%$ ,  $25 \text{ }^\circ\text{C}$ ) oscillatory shear rheology of PNP hydrogels comprising 1 wt% HPMC- $\text{C}_{12}$  and 10 wt% PEG-PLA NPs at monthly timepoints over a 6 month storage period. j) Step-strain measurements of PNP hydrogels with high strains (destructive; 750%) and low strains (restorative; 0.5%) to characterize the extent and rate of stationary self-healing over a 6 month time period. k) Steady shear rheology of PNP hydrogels demonstrating retained, highly shear-thinning behavior over a 6 month time period.

## 2.2. In Vivo Efficacy in a Rodent Model of Peritoneal Adhesions

In this report we expand upon our previous studies by investigating the use of PNP hydrogels for prevention of adhesions in an abdominal surgery indication.<sup>[22]</sup> We utilized a published rodent peritoneal ischemic button model that was demonstrated to be more effective at generating a robust adhesion response compared to other standard abdominal adhesion models.<sup>[33]</sup> The inflammation and tissue damage occurring in this model reproducibly generated severe peritoneal adhesions. A midline incision was performed and four ischemic buttons were created on each side of the peritoneal wall (i.e., a total of 8 ischemic buttons per animal). The ischemic buttons were created in rodents via a stick tie suture technique in order to create a region of ischemia along the peritoneal wall (Figure 3a–i). Immediately following ischemic button induction, rats received either i) PNP hydrogel comprising 1 wt% HPMC and 10 wt% PEG-PLA NPs (800  $\mu\text{L}$ ), ii) PNP hydrogel comprising 2 wt% HPMC and 10 wt% PEG-PLA NPs (800  $\mu\text{L}$ ), iii) a commercially available adhesion barrier, Seprafilm (4  $\text{cm}^2$ ), or iv) no treatment prior to closing the

midline incision. Treatments were applied directly over the ischemic buttons that were created on the peritoneal surface. Rats were sacrificed 4 weeks later to evaluate the anti-adhesive efficacy of our PNP hydrogel adhesion barrier. A midline incision was performed to visualize the extent of adhesion formation prior to blunt dissection (Figure 3b-i,c-i,d-i). Blunt dissection was utilized to assess the in vivo efficacy of the adhesion barrier technologies on the severity and adherence of adhesions to the peritoneal wall (Figure 3b-ii,c-ii,d-ii). Using videos, images, and the physical dissection process, adhesion scores were assigned via a double blinded clinical scoring system on a scale from 0 to 5 (Table 1, Figure 3e). In this clinical scoring system, a score of zero indicates no adhesions and a score of five indicates a high incidence of severe, tightly adhered, vascularized adhesions. Finally, adhesions were lysed and the peritoneal wall was preserved for histological analysis.

In the untreated control group, the adhesions were tightly adhered to the peritoneal wall (Figure 3b-i,b-ii), presenting an adhesion score of  $2.75 \pm 1.16$  requiring the use of scissors since the adhesions were unable to be removed with instrument



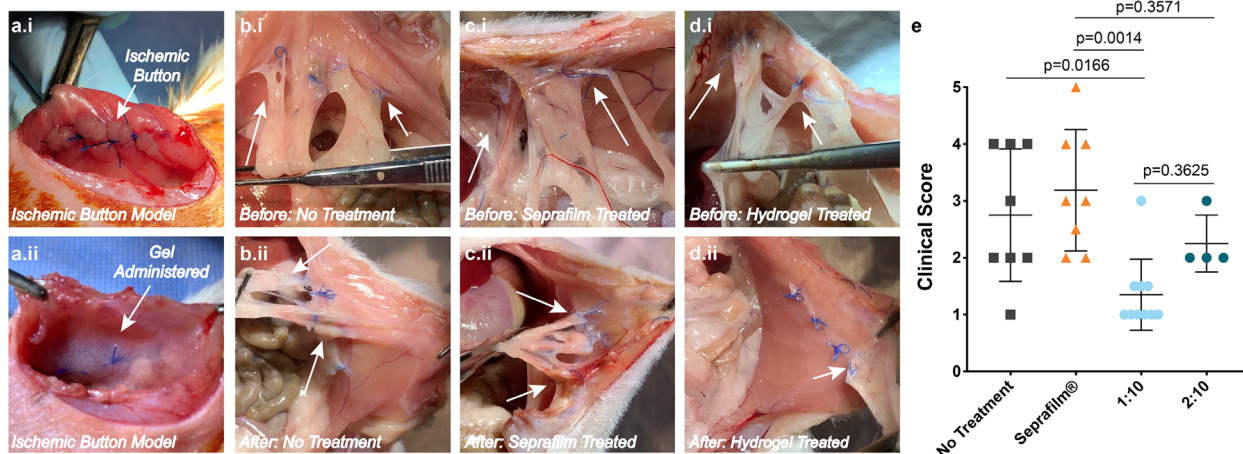


**Figure 3.** a-i) Representative image of the induction of peritoneal ischemic buttons prior to treatment administration. a-ii) Representative image of PNP 1:10 hydrogel administered over the peritoneal ischemic buttons to provide a PNP 1:10 hydrogel adhesion barrier. b-i) Representative image of an untreated peritoneal wall 4 weeks after the induction of peritoneal ischemic buttons, prior to dissection. b-ii) Representative image of an untreated peritoneal wall after blunt dissection indicating tightly adhered adhesions unable to be lysed with blunt dissection. c-i) Representative image of a Sefrafilm treated peritoneal wall 4 weeks after the induction of peritoneal ischemic buttons, prior to dissection. c-ii) Representative image of a Sefrafilm treated peritoneal wall after blunt dissection indicating tightly adhered adhesions unable to be lysed with blunt dissection. d-i) Representative image of a PNP 1:10 hydrogel treated peritoneal wall 4 weeks after the induction of peritoneal ischemic buttons, prior to dissection. d-ii) Representative image of the in vivo efficacy of the PNP 1:10 hydrogel after blunt dissection of the peritoneal wall indicating loosely adhered adhesions. The white arrows in images (c–h) indicate adhesions. e) Double-blinded clinical scoring of adhesion formation 4 weeks following induction of the peritoneal ischemic buttons. Data presented as mean  $\pm$  s.d. ( $n > 4$ ). PNP hydrogel formulation is comprised of 1 wt% HPMC-C<sub>12</sub> and 10 wt% PEG-PLA NPs (1:10) or 2 wt% HPMC-C<sub>12</sub> and 10 wt% PEG-PLA NPs (2:10). Statistical significance was determined using a one-way analysis of variance (ANOVA) with multiple comparisons against untreated controls.

**Table 1.** Adhesion Scoring System.

| Score | Peritoneal Adhesion  |
|-------|--|
| 0     | No adhesions   |
| 1     | Few thin, filmy adhesions, loosely adhered to the peritoneal wall          |
| 2     | Numerous thin adhesions, loosely adhered to the peritoneal wall            |
| 3     | Moderate adhesions, moderately adhered to the peritoneal wall              |
| 4     | Dense adhesions, tightly adhered to the peritoneal wall                    |
| 5     | Very dense, vascularized adhesions, tightly adhered to the peritoneal wall |

manipulation or blunt dissection alone. The commercial adhesion barrier treatment group presented with an adhesion score of  $3.18 \pm 1.07$ , which was not statistically different from that of the control groups (Figure 3c-i, c-ii). Animals treated with the PNP 1:10 hydrogel exhibited a lower overall adhesion score ( $1.35 \pm 0.63$ ) and any adhesions that formed were easily removed from the peritoneal wall using blunt dissection via forceps. These results suggest that the viscoelastic PNP hydrogel adhesion barrier significantly reduced the incidence and severity of adhesions following abdominal surgery suggesting more facile dissection in comparison to the untreated and commercial control groups. The PNP 2:10 hydrogel formulation yielded an adhesion score of  $2.75 \pm 0.5$ , similar to untreated animals, indicating that an optimal range of yield stress and storage moduli exists for these materials, whereby enhanced performance is observed for the PNP 1:10 hydrogel formulation despite it being a softer material, corroborating our previous reports on adhesion prevention in cardiothoracic surgery.<sup>[22]</sup> These observations suggest that PNP hydrogel formulations like the PNP 2:10 formulation, which

exhibit greater yield stress values and increased mechanical stiffness compared to the top-performing PNP 1:10 formulation, may not consistently result in effective adhesion barrier function. We hypothesize that the variable efficacy observed for formulations with more robust mechanical properties, similar to the PNP 2:10 formulation, likely arises from these materials becoming dislodged from the site of application due to adhesive failure on account of the stiffness of these materials.

### 2.3. PNP Hydrogel Retention at the Site of Application

The retention timeframe of the top-performing PNP 1:10 hydrogel formulation was investigated in the peritoneal space using fluorescently labeled PNP 1:10 hydrogels. In these studies, animals were treated with an NIR-797-labeled PNP 1:10 hydrogel and imaged on day 0, 1, 2, 7, 9, 14, and 21 (Figure 4). Following administration, hydrogels exhibited intense signal in the peritoneal space at the site of application (Figure 4a). The signal steadily declined over the course of the study, indicating that the hydrogels persisted locally in the peritoneal space for approximately 2 weeks (Figure 4b). Since the reported pathophysiology for adhesion formation occurs 7–14 days following surgery, this timeframe is beneficial for continual coverage and adhesion prevention in the abdominal cavity, corroborating the observations made during the efficacy studies described above.

### 2.4. Histological Examination and PNP Hydrogel Biocompatibility

To assess the extent of local fibrin and collagen deposition, fibrosis, and inflammation within the peritoneal wall following

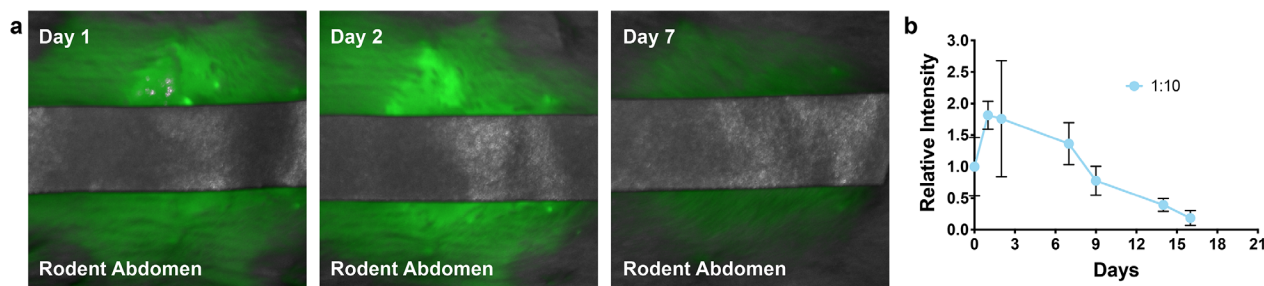


**Figure 4.** a) Pearl live imaging of NIR-797 labeled PNP hydrogel administered to the peritoneal wall following a midline incision and induction of peritoneal ischemic buttons. b) In vivo retention over time of the PNP 1:10 hydrogel indicated by relative fluorescence intensity.

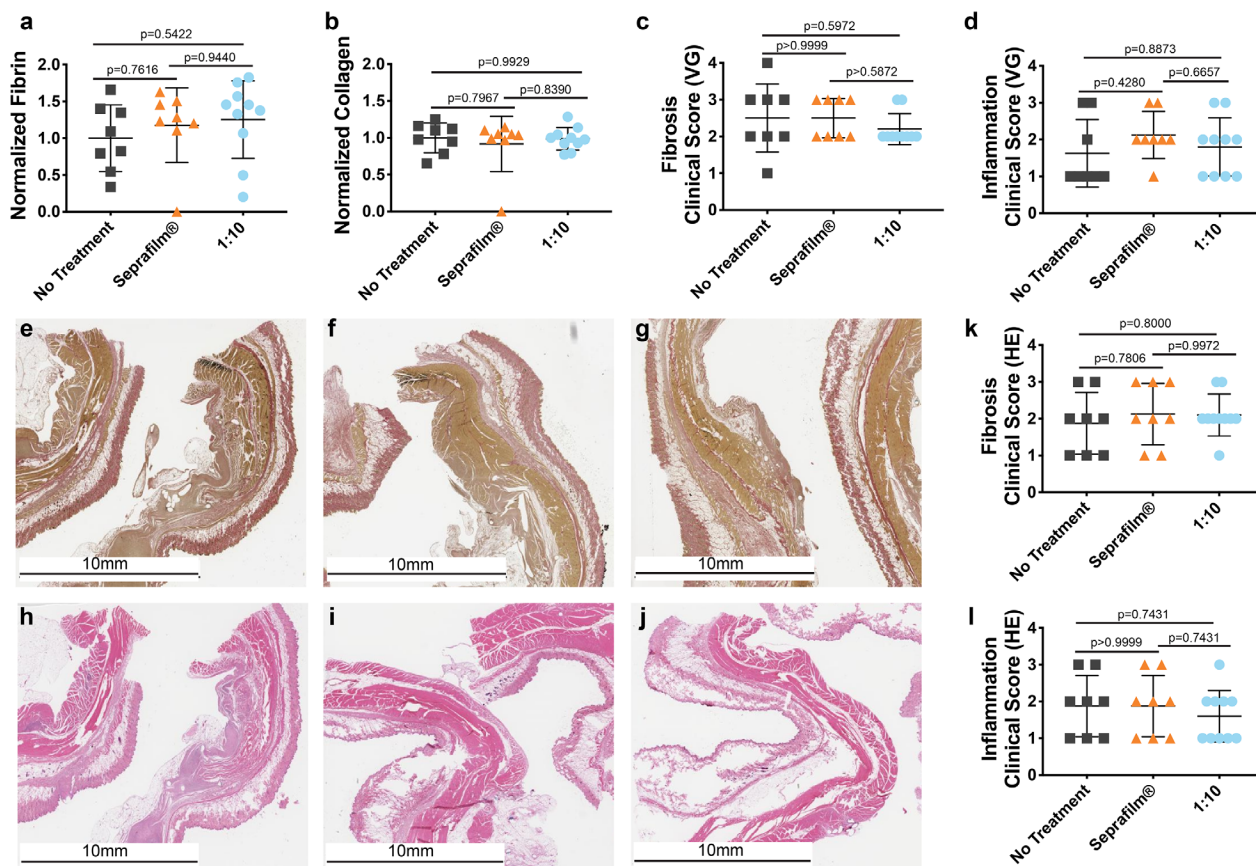


**Figure 5.** a) Normalized fibrin quantification in peritoneum tissue sections stained with Van Gieson 4 weeks following induction of ischemic buttons. b) Normalized collagen quantification in peritoneum tissue sections stained with Van Gieson 4 weeks following induction of ischemic buttons. c) Pathologist assigned clinical scores for tissue fibrosis in peritoneum section stained with Van Gieson. d) Pathologist assigned clinical scores for tissue inflammation in peritoneum section stained with Van Gieson. e–g) Representative images of Van Gieson stained peritoneum tissue sections from the untreated, Seprafilm, and PNP hydrogel 1:10 treated groups, respectively. Fibrin (yellow). Collagen (red). h–j) Representative images of Hematoxylin and Eosin stained peritoneum tissue sections from the untreated, Seprafilm, and PNP hydrogel 1:10 treated groups, respectively. Fibrin (yellow). Collagen (red). k) Pathologist assigned clinical scores for tissue fibrosis in peritoneum section stained with Hematoxylin and Eosin. l) Pathologist assigned clinical scores for tissue inflammation in peritoneum section stained with Hematoxylin and Eosin. Statistical significance was determined using a one-way analysis of variance (ANOVA) with multiple comparisons against untreated controls. VG, Van Gieson; HE, Hematoxylin and Eosin.

the induction of peritoneal ischemic buttons, a blinded pathologist examined Van Gieson (VG) and Hematoxylin and Eosin (HE) stained sections of peritoneal wall from every rodent in each treatment group (untreated, Seprafilm, and PNP 1:10 hydrogel,  $n > 8$ ). Van Gieson staining reveals the presence of both fibrin and collagen within a tissue and the staining analysis re-

vealed no statistical difference between the quantified collagen and fibrin deposition between the untreated, Seprafilm treated, and PNP 1:10 hydrogel treated animals (Figure 5a–b,e–g). Additionally, the pathologist assigned clinical scores for sample fibrosis and inflammation ranging from 0 (normal) to 4 (severe change in >50% tissue) (Figure 5c–d,e–g). The Van Gieson tissue

sections also revealed no statistical difference between controls and the PNP 1:10 hydrogel treated group. Similarly, pathologist-assigned clinical scores for sample fibrosis and inflammation in tissue sections stained with Hematoxylin and Eosin corroborated the clinical scores assigned for the Van Gieson stained samples and revealed no statistical significance between the untreated, Seprafilm treated, and PNP 1:10 hydrogel treated groups (Figure 5h–l). These results indicate consistent inflammation and fibrosis resulting from controlled peritoneal ischemic button induction, suggesting all animals underwent similar inflammatory responses and tissue necrosis, thereby initiating a similar and reproducible local adhesion formation cascade following each surgery.

Additionally, we sought to investigate the biocompatibility of the PNP 1:10 hydrogel adhesion barrier in the peritoneal space. For this study, female rats underwent a sham surgery and received administration of 800  $\mu$ L of PNP hydrogel in the peritoneal space. At 4-weeks post-surgery the rodents were submitted to a pathologist for gross necropsy and histological analysis of surrounding tissues. There were no significant findings among any of the tissues examined by the pathologist. Noted findings consisted of minimal vacuolated macrophages observed around the trabecular sinuses of the lymph node and within the marginal zone of the spleen in all hydrogel treated rodents; however, this was associated with normal hydrogel clearance and is not considered adverse. Complete blood count and blood chemistry panels also indicated no significant abnormalities (Figure S1, Supporting Information).

### 3. Conclusion

This study demonstrates a new surgical arena that can benefit from the use of a supramolecular PNP hydrogel adhesion barrier. The use of a viscoelastic adhesion barrier with dynamic, transient crosslinks is an innovative approach that is distinct from previously reported systems based on covalent hydrogels, films, or fabric. Additionally, this approach improves upon current clinical options consisting of film or fabric adhesion barriers. This PNP hydrogel formulation exhibits shear-responsive rheological properties that are crucial for simple administration by spraying onto the surface of interest (i.e., peritoneal wall), sustained local retention, and robust reduction in adhesion severity. Furthermore, this viscoelastic adhesion barrier is simple to scale and demonstrates stable mechanical properties under 4 °C storage conditions for at least 6 months, further enhancing the therapeutic potential of these materials.

The PNP hydrogel adhesion barrier is based on distinct mechanical properties providing for optimal clinical efficacy in adhesion prevention. The material is capable of viscous flow under applied shear (e.g., spraying) enabling uniform coverage over the peritoneal tissue vulnerable to adhesion formation. Once the applied shear is removed, the material rapidly forms a solid-like barrier that adheres to the peritoneal wall, preventing the material from becoming dislodged and maintaining a physical separation of the tissues in the peritoneal cavity. Due to the transient and dynamic nature of the PNP adhesion barrier crosslinks, this innovative adhesion barrier demonstrates rapid, reversible transition between viscous flow and solid-like state. This transition allows for simultaneous viscous flow between neighboring tissues and

physical separation while remaining adhered to tissue, which is crucial for maintaining natural body movement while preventing dislodging of the material. Our in vivo studies demonstrate the therapeutic benefit of these mechanical properties in a small animal model of abdominal adhesions. Treatment with the PNP hydrogel adhesion barrier resulted in significantly reduced clinical adhesion scores that attribute to decreased incidence and severity of adhesion formation.

These PNP hydrogel materials are particularly attractive for this application due to their facile administration by simple spraying or spreading using standard equipment, or through minimally invasive catheter delivery, coupled with their high degree of efficacy and excellent biocompatibility. Continued studies investigating a range of mechanical properties should be conducted to optimize the PNP hydrogel system for further reduction of abdominal adhesions following peritoneal surgery. Additionally, promising hydrogel formulations should be investigated in large animal models of abdominal adhesions, which theoretically generate more clinically relevant adhesions that more closely mimic human abdominal surgeries, to explore the potential for clinical application. We also believe our PNP hydrogel adhesion barrier system can be effective in surgeries beyond the abdominal and cardiac systems, including laparoscopic surgeries where adhesions present a significant clinical challenge.

In summary, the PNP hydrogel adhesion barrier reported here resulted in a significant reduction in the severity and incidence of peritoneal adhesions using a robust small animal model of peritoneal adhesion formation. This treatment approach has the potential to positively impact patients and prevent adhesion formation as a result of surgery of any kind in any part of the body. Overall, this work establishes a proof of concept translation across surgery indications and demonstrates an adhesion barrier system that is simple to deploy, stable over extended timeframes, and successfully prevents post-operative adhesions.

### 4. Experimental Section

**Materials:** HPMC, *N,N*-diisopropylethylamine (Hunig's base), hexanes, diethyl ether, *N*-methylpyrrolidone (NMP), dichloromethane (DCM), lactide (LA), and diazobicylcoundecene (DBU) were purchased from Sigma Aldrich as used as received.

**Synthesis of HPMC-C<sub>12</sub>:** HPMC-C<sub>12</sub> was prepared according to literature preps and the methods are reproduced here.<sup>[23]</sup> HPMC (1.0 g) was dissolved in NMP (40 mL) by stirring at 80 °C for 1 h. Once the solution cooled to room temperature, 1-dodecylisocyanate (105 mg, 0.5 mmol) and *N,N*-diisopropylethylamine (catalyst,  $\approx$ 3 drops) were dissolved in NMP (5.0 mL). This solution was added to the reaction mixture, which was then stirred at room temperature for 16 h. This solution was then precipitated from acetone and the polymer was recovered by filtration, dried under vacuum at room temperature for 24 h and weighed, yielding functionalized HPMC-C<sub>12</sub> as a white amorphous powder.

**Synthesis of PEG-b-PLA:** PEG-PLA was prepared according to literature preps and the methods are reproduced here.<sup>[23]</sup> PEG (0.25 g, 4.1 mmol; Aldrich) and DBU (10  $\mu$ L, 10.6 mg; 1.0 mol% relative to LA) were dissolved in DCM (1.0 mL). LA (1.0 g, 6.9 mmol) was dissolved in DCM (3.0 mL) with mild heating. The LA solution was added rapidly to the PEG/DBU solution and was allowed to be stirred for 10 min. The reaction mixture was quenched and precipitated by 1:1 hexane and ethyl ether solution. PEG-PLA was collected and dried under vacuum.

**PEG-b-PLA Nanoparticle (NP) Preparation:** PEG-PLA NPs were prepared according to literature preps and the methods are reproduced here.<sup>[23]</sup> A solution of PEG-PLA in DMSO (50 mg mL<sup>-1</sup>) was added



dropwise to water ( $80 \mu\text{L min}^{-1}$ ) under a high stir rate. NPs were purified by ultracentrifugation over a filter (molecular weight cut-off of 10 kDa; Millipore Amicon Ultra-15) followed by resuspension in water to a final concentration of  $150 \text{ mg mL}^{-1}$ . NP size and dispersity were characterized by DLS.

**PNP Hydrogel Preparation:** PNP hydrogels were prepared by first dissolving HPMC polymers in water (3 wt%) with stirring and mild heating. PEG-PLA NPs were prepared according to the method described above and were concentrated to 15 wt% solutions. HPMC polymer solution (150 mL) and NP solution (300 mL) were added together and mixed well by vortex (some samples were mildly centrifuged to remove bubbles arising from mixing) to create the PNP hydrogel formulation.

**PNP Hydrogel Characterization:** Rheological characterization was performed using a TA Instruments AR-G2 controlled-stress rheometer fitted with a Peltier stage. All measurements were performed using a 20-mm plate and analyzed using TA Instruments TA Orchestrator software.

**NIR 797-Labeled HPMC-C<sub>12</sub> Preparation:** An 8 mL vial was charged with N-[(1R,8S,9S)-bicyclo[6.1.0]non-4-yn-9-ylmethoxycarbonyl]-1,8-diamino-3,6-dioxaoctane (2.06 mg, 6.40 mol) and NIR-797 isothiocyanate (7.7 mg, 8.8 mol) and dissolved in 50 mL N-methyl pyrrolidone (NMP). The mixture was incubated at room temperature for 30 min. 100 mg of N3-PEG-PLA in 0.5 mL in NMP was added and the mixture incubated for 72 h at room temperature. The modified PEG-PLA was recovered by removal of NMP by sequential extraction with diethyl ether in the reaction vial. The moist precipitated polymer was dissolved in a minimal amount of acetone, approximately 0.3 mL, and reprecipitated by the addition of diethyl ether to the vial. The polymer was further purified by dissolving it in acetone and passing it through a silica plug in a glass Pasteur pipette, using acetone, followed by removal of acetone in vacuo to recover the purified modified polymer.

**Rodent Peritoneal Adhesion Model:** All animal procedures were performed according to Stanford Animal Care and Use Committee approved protocols. For in vivo efficacy studies, 15 adult female Wistar Rats (200–250 g, Charles River) underwent ligation of the peritoneal wall generating ischemic buttons. Rats were sedated under 3% inhaled isoflurane (Fluriso, VetOne). The rats were injected with Buprenorphine SR ( $0.3\text{--}1.2 \text{ mg kg}^{-1}$ ) subcutaneously (SQ) and their abdomen were shaved for pre-surgical preparation. The animal was then intubated with a 16 G angiocatheter and ventilated at 80 breaths/min,  $1 \text{ L min}^{-1} \text{ O}_2$ , a PIP of 35 cm H<sub>2</sub>O, PEEP of 5, a 33:66 I:E ratio, and a 2–3 mL tidal volume (Hallowell EMC Pitt). Once stabilized on the ventilator, isoflurane was maintained lower at 1–2%. The abdominal area was prepped with Betadine followed by a midline incision along the abdomen for entry into the abdominal cavity.

The ischemic buttons were made by pinching off a small portion of the parietal peritoneum with a right angle surgical instrument. A stick-tie was used to ligate the pinched peritoneum. In accordance with the Johnson and Johnson Company, Wound Closure Manual, the stick tie is used for ligation of a deep structure or large vessel. In this instance, an RB-2 4-0 prolene suture was passed through the pinched tissue for anchorage, and the suture wrapped around the button causing ischemia of the tissue. Finally, the suture was secured in place with several square knots. Four buttons were created on each side, spanning the length of the incision, for a total of eight buttons per animal. Immediately following ischemic button formation, the animals received administration of PNP hydrogel (800  $\mu\text{L}$ ); Seprafilm (commercially available standard-of-care adhesion barriers; 4 cm<sup>2</sup>); or no treatment. A subset of animals was administered NIR-797 tagged PNP hydrogel for the in vivo retention study. The muscle layers were then closed with an over and over running suture using RB-2 4-0 prolene. The skin was closed using simple interrupted stitches using RB-2 4-0 prolene suture. Finally, to protect the incision, Dermabond was applied to the incision and the animals were allowed to recover.

**In Vivo Retention Study:** A subset of animals ( $n = 3$ ) were administered NIR-797 tagged PNP hydrogels. Animals were imaged on days 0, 1, 2, 7, 9, 14, and 16 using the Pearl Trilogy Small Animal Imaging System (LI-COR Biosciences).

**Biocompatibility Study:** A subset of animals ( $n = 3$ ) were used to test the biocompatibility of the PNP hydrogel. Similar to the other animals, a midline incision of the abdomen was made, and the hydrogel applied

to the abdominal cavity. 4 weeks post-surgery, the rats were submitted to a pathologist for gross necropsy. Complete blood chemistry and complete blood panels were also performed. The tissues were explanted for gross study and tissues were further cut, sectioned, and stained for Hematoxylin and Eosin (H&E). An independent and blinded pathologist examined each tissue: liver, spleen, kidney, adrenal gland, salivary gland, thymus, pancreas, heart, lung, trachea, esophagus, thyroid gland, tongue, lymph nodes, testes, accessory sex glands, eyes, cerebellum, cerebrum, stomach, small intestine, large intestine, and peritoneal wall.

**Histology:** At 4 weeks post-surgery, rats were anesthetized under 4% isoflurane and euthanized by cervical dislocation. A midline incision of the abdomen was made along the original suture line, if still visible, to open the skin and the muscle layers. Video recording began immediately after opening of the muscle layers in order to capture the adhesions throughout and across the abdominal cavity and fully assess efficacy of possible treatment. After an initial video was captured, a blinded investigator further opened the abdominal cavity to examine individual adhesions for scoring. Adhesions scores were assigned for both the right and left sides of the abdominal cavity and subsequently plotted as separate data points. A double-blinded clinical scoring system, ranging on a scale from 0–5, was used to evaluate adhesion formation: no adhesions (0), a few filmy adhesions; loosely adhered to the peritoneal wall (1), numerous filmy adhesions; loosely adhered to the peritoneal wall (2), moderate adhesions; moderately adhered to the peritoneal wall (3), dense adhesions; tightly adhered to the peritoneal wall (4) and very dense, vascularized adhesions; tightly adhered to the peritoneal wall (5).

After a score was given, the area around the buttons was excised and placed in room temperature 4% paraformaldehyde for 48 h. Following fixation, samples were cut, arranged in paraffin processing tissue cassettes and placed into 70% ethanol stored at room temperature. Samples were sectioned and stained with Van Gieson stain or Hematoxylin and eosin stain. Following sectioning and staining, a veterinary pathologist blinded to the treatment groups analyzed each section for signs of fibrosis and inflammation. Scores for fibrosis and inflammation were assigned the following criteria: score 0 (normal); score 1 (minimal change in <10% tissue); score 2 (mild change in 10–25% tissue); score 3 (moderate change in 25–50% tissue); score 4 (severe change in >50% tissue). Automated image analysis, using HALO software (Indica Labs), was used to analyze the Van Gieson stained slides for quantification of fibrin and collagen. The presence of fibrin (red stain) and collagen (yellow stain) was analyzed by signal intensity using whole slide images.

**Statistical Analysis:** All results are expressed as a mean  $\pm$  standard deviation (s.d.). Comparison between two groups were conducted by a two-tailed Student's *t*-test. One-way ANOVA test was used for comparison across multiple groups. Statistical significance was considered as  $p < 0.05$ .

**Animal Randomization:** Animal cages were housed in a random order on the shelf. Physical randomization occurred before each operation using a random number generator. The adhesion scoring was done in a random order, with the surgeon and clinical scorer being blinded to the treatment groups.

**Animal Care:** Female Wistar rats were obtained from Charles River Laboratories (Wilmington, MA) and allowed to acclimate in the holding facility for several days before surgery. All procedures were carried out according to a Stanford University Administrative Panel on Laboratory Animal Care (APLAC) approved protocol (Protocol #33032), which is an Association for the Assessment and Accreditation of Laboratory Animal Care (AAALAC International) approved program.

## Supporting Information

Supporting Information is available from the Wiley Online Library or from the author.

## Acknowledgements

This work was made possible by the financial support from the Stanford-Coulter Translational Research Grant (E.A.A. and Y.J.W.), the Ameri-



can Heart Association Predoctoral Fellowship (L.M.S.), and the Stanford Interdisciplinary Graduate Fellowship (L.M.S.). The authors thank the Bogoy laboratory for the use of the Pearl instrument; Stanford Animal Histology Services, and Histowiz for assistance with histological analysis.

## Conflict of Interest

L.M.S., Y.J.W. and E.A.A. are listed as inventors on a patent application describing the technology reported in this manuscript. The other authors declare no conflict of interest.

## Keywords

biomaterials, hydrogels, post-operative adhesions, surgery, viscoelastic

Received: October 27, 2020

Revised: December 12, 2020

Published online:

- 
- [1] W. Arung, M. Meurisse, O. Detry, *World J. Gastroenterol.* **2011**, *17*, 4545.
- [2] M. P. Diamond, M. L. Freeman, *Hum. Reprod. Update* **2001**, *7*, 567.
- [3] C. I. W. Lauder, G. Garcea, A. Strickland, G. J. Maddern, *Dig. Surg.* **2010**, *27*, 347.
- [4] M. A. Weibel, G. Majno, *Am. J. Surg.* **1973**, *126*, 345.
- [5] G. S. diZerega, J. D. Campeau, *Hum. Reprod. Update* **2001**, *7*, 547.
- [6] T. Ito, Y. Yeo, C. B. Highley, E. Bellas, C. A. Benitez, D. S. Kohane, *Biomaterials* **2007**, *28*, 975.
- [7] Y. Yeo, M. Adil, E. Bellas, A. Astashkina, N. Chaudhary, D. S. Kohane, *J. Control. Release* **2007**, *120*, 178.
- [8] A. Hirschelmann, G. Tchartchian, M. Wallwiener, A. Hackethal, R. L. De Wilde, *Arch. Gynecol. Obstet.* **2012**, *285*, 1089.
- [9] E. Ergul, B. Korukluoglu, *Int. J. Surg.* **2008**, *6*, 253.
- [10] V. Sikirica, B. Bapat, S. D. Candrilli, K. L. Davis, M. Wilson, A. Johns, *BMC Surg.* **2011**, *11*, 13.
- [11] T. Tulandi, M. Agdi, A. Zarei, L. Miner, V. Sikirica, *Am. J. Obstet. Gynecol.* **2009**, *201*, P56.E1.
- [12] M. P. Diamond, E. L. Burns, B. Accomando, S. Mian, L. Holmdahl, *Gynecol. Surg.* **2012**, *9*, 237.
- [13] A. S. Sawhney, C. P. Pathak, J. J. van Rensburg, R. C. Dunn, J. A. Hubbell, *J. Biomed. Mater. Res.* **1994**, *28*, 831.
- [14] T. Hoare, Y. Yeo, E. Bellas, J. P. Bruggeman, D. S. Kohane, *Acta Biomater* **2014**, *10*, 1187.
- [15] D. A. Grainger, W. R. Meyer, A. H. DeCherney, M. P. Diamond, *J. Gynecol. Surg.* **1991**, *7*, 97.
- [16] L. Li, N. Wang, X. Jin, R. Deng, S. Nie, L. Sun, Q. Wu, Y. Wei, C. Gong, *Biomaterials* **2014**, *35*, 3903.
- [17] W. Zhu, L. Gao, Q. Luo, C. Gao, G. Zha, Z. Shen, X. Li, *Polym. Chem.* **2014**, *5*, 2018.
- [18] M. Chan, H. J. L. Brooks, S. C. Moratti, L. R. Hanton, J. D. Cabral, *Int. J. Mol. Sci.* **2015**, *16*, 13798.
- [19] L. Song, L. Li, T. He, N. Wang, S. Yang, X. Yang, Y. Zeng, W. Zhang, L. Yang, Q. Wu, C. Gong, *Sci. Rep.* **2016**, *6*, 37600.
- [20] Y. Yang, X. Liu, Y. Li, Y. Wang, C. Bao, Y. Chen, Q. Lin, L. Zhu, *Acta Biomater* **2017**, *62*, 199.
- [21] T. Banasiewicz, K. Horbacka, J. Karoń, S. Malinger, F. Antos, S. Rudzki, Z. Kala, Z. Stojcev, J. Kössi, P. Krokowicz, *Wideochir Inne Tech Maloinwazyjne* **2013**, *8*, 301.
- [22] L. M. Stapleton, A. N. Steele, H. Wang, H. Lopez Hernandez, A. C. Yu, M. J. Paulsen, A. A. A. Smith, G. A. Roth, A. D. Thakore, H. J. Lucian, K. P. Thorerow, S. W. Baker, Y. Tada, J. M. Farry, A. Eskandari, C. E. Hironaka, K. J. Jaatinen, K. M. Williams, H. Bergamasco, C. Marschel, B. Chadwick, F. Grady, M. Ma, E. A. Appel, Y. J. Woo, *Nat. Biomed. Eng.* **2019**, *3*, 611.
- [23] E. A. Appel, M. W. Tibbitt, M. J. Webber, B. A. Mattix, O. Veiseh, R. Langer, *Nat. Commun.* **2015**, *6*, 6295.
- [24] A. C. Yu, A. A. A. Smith, E. A. Appel, *Mol. Syst. Des. Eng.* **2020**, *5*, 401.
- [25] O. S. Fenton, M. W. Tibbitt, E. A. Appel, S. Jhunjhunwala, M. J. Webber, R. Langer, *Biomacromolecules* **2019**, *20*, 4430.
- [26] A. K. Grosskopf, G. A. Roth, A. A. A. Smith, E. C. Gale, H. L. Hernandez, E. A. Appel, *Bioeng. Transl. Med.* **2020**, *5*, e10147.
- [27] G. A. Roth, E. C. Gale, M. Alcántara-Hernández, W. Luo, E. Axpe, R. Verma, Q. Yin, A. C. Yu, H. L. Hernandez, C. L. Maikawa, A. A. A. Smith, M. M. Davis, B. Pulendran, J. Idoyaga, E. A. Appel, *BioRxiv:2020.05.26.117465* **2020**.
- [28] H. L. Hernandez, A. K. Grosskopf, L. M. Stapleton, G. Agmon, E. A. Appel, *Macromol. Biosci.* **2019**, *19*, 1800275.
- [29] M. J. Webber, E. A. Appel, E. W. Meijer, R. Langer, *Nat. Mater.* **2016**, *15*, 13.
- [30] J. L. Mann, A. C. Yu, G. Agmon, E. A. Appel, *Biomater. Sci.* **2017**, *6*, 10.
- [31] E. A. Appel, J. del Barrio, X. J. Loh, O. A. Scherman, *Chem. Soc. Rev.* **2012**, *41*, 6195.
- [32] C. L. Maikawa, A. Sevit, B. Lin, R. J. Wallstrom, J. L. Mann, A. C. Yu, R. M. Waymouth, E. A. Appel, *J. Polym. Sci. A, Polym. Chem.* **2019**, *57*, 1322.
- [33] B. Kraemer, C. Wallwiener, T. K. Rajab, C. Brochhausen, M. Wallwiener, R. Rothmund, *Biomed Res. Int.* **2014**, *2014*, 435056.